

## Article

# Cellulose-Graphene Bifunctional Paper Conservation Materials: For Reinforcement and UV Aging Protection

Peng Tian <sup>1,\*</sup>, Meirong Shi <sup>2</sup>, Jingmin Hou <sup>2</sup> and Peng Fu <sup>2,\*</sup><sup>1</sup> School of Art and Media, Xi'an Technological University, Xi'an 710021, China<sup>2</sup> Shaanxi Institute for the Preservation of Culture Heritage, Xi'an 710075, China

\* Correspondence: tpmx1982@126.com (P.T.); fupeng@snnu.edu.cn (P.F.)

**Abstract:** Paper artifacts have unique cultural and historical values. However, over time, many paper artifacts appear with disease characteristics such as embrittlement and photoaging, losing the most fundamental function of the literature archive. The reinforcement handling of degraded paper artifacts is, therefore, a necessary measure to extend their service life, the key to which lies in the reinforcement and prevention of photoaging. This paper intended to use graphene oxide (GO) as a UV protective agent, carboxymethyl cellulose (CMC) as a reinforcement, and polyethyleneimine (PEI) as a modifier. In this work, the amino-modified graphene oxide carboxymethyl cellulose composite (CMC-aGO) was prepared by chemical modification, which was used as bifunctional paper protection material with anti-ultraviolet and reinforcement. It showed excellent performance in both tensile strength testing and UV resistance testing. The CMC-aGO raw material is low cost, colorless, transparent, simple to synthesize, convenient to operate, and is an excellent conservation material with dual functions of UV aging protection and paper reinforcement.

**Keywords:** graphene oxide; carboxymethyl cellulose; UV aging protection; paper reinforcement



**Citation:** Tian, P.; Shi, M.; Hou, J.; Fu, P. Cellulose-Graphene Bifunctional Paper Conservation Materials: For Reinforcement and UV Aging Protection. *Coatings* **2023**, *13*, 443. <https://doi.org/10.3390/coatings13020443>

Academic Editor: Csaba Balázsi

Received: 11 January 2023

Revised: 9 February 2023

Accepted: 14 February 2023

Published: 15 February 2023



**Copyright:** © 2023 by the authors. Licensee MDPI, Basel, Switzerland. This article is an open access article distributed under the terms and conditions of the Creative Commons Attribution (CC BY) license (<https://creativecommons.org/licenses/by/4.0/>).

## 1. Introduction

Paper cultural relics, in the form of archives, book drawings, newspapers, literature, etc., are commonly used to record valid information. As one of the important carriers of culture, science, politics, education, and economy, paper cultural relics have an immeasurable value of their own existence [1–4]. However, over time, some paper cultural relics due to natural aging, acidification, ultraviolet, and other internal and external factors lead to diseases such as yellowing, crispness, and mildew, which endanger the potential value of paper itself. The main components of paper are cellulose, lignin, and hemicellulose, as well as additives (starch, minerals, synthetic polymers, etc.) [5–9]. The aging factors include internal and external factors. Internal factors include the hydrolysis and oxidation of cellulose, which decreases the van der Waals force and hydrogen bond force between cellulose molecules, resulting in decreased intermolecular polymerization and paper mechanical strength. Extrinsic factors of aging in paper artifacts include temperature, humidity, sunlight, air pollution, microbial influences, etc. [2]. Among them, light is extremely hazardous to paper and literal pigments. UV light in daylight exposure is highly destructive. It has the characteristics of long wavelength and high energy, which may cause the change in high energy state and the transfer of energy between the paper fiber and pigment molecules, making it undergo a series of photochemical reactions [9–12]. This caused the paper fiber structure to oxidatively degrade, making the paper polymerization degree overall decline, and making its mechanical properties less stable, eventually causing irreversible damage to the paper. Therefore, developing reinforcement materials with UV aging resistance is of great significance to protect paper-based artifacts [13–15].

In the field of paper-based cultural relics protection, organic polymer materials have become a research hotspot due to their excellent reinforcement effect, simple operation, and

rapid effect, mainly including synthetic polymer materials and natural polymer materials. Compared with synthetic polymer materials, natural polymer materials stand out for their advantages in safety, environmental friendliness, compatibility with paper, and reversibility, and become a hotspot of competitive research among researchers for the protection of paper artifacts. Cellulose is the most abundant and inexhaustible renewable resource in nature. It has the advantages of low cost, high quality, environmental protection, and safety [16,17]. In addition, cellulose itself is the main component of paper, and its physical and chemical properties are similar. When external environment conditions change, there is no stress between cellulose and paper fiber materials, which causes secondary damage to the paper. Basically, to meet the requirements of paper cultural relics protection for reinforcement materials, the principle of “repair the old as the old, keep the original appearance” should be followed and may also have the characteristics of aging resistance, reversibility, and paper compatibility.

Among many paper reinforcement materials, carboxymethylcellulose (CMC), as a water-soluble cellulose derivative, has excellent water solubility, viscosity, diffusibility, stability, and environmental friendliness [18]. It can be used for paper reinforcement and is widely used in this field. CMC molecules are intertwined due to their special long-chain structure [19]. The film formed by CMC has excellent toughness, flexibility, and transparency and can block oil and water. In addition, this weak alkaline solution can neutralize acidic substances in the paper and slow the progress of paper acidification and aging. Meanwhile, a large number of functional groups in the CMC structure are able to interact with hydroxyl or hydrogen bonds in the cellulose structure of the paper and are able to form a stable fibrous network on the surface of the paper, thereby playing a strengthening role [20,21]. Chen et al. found that the carboxymethyl cellulose-modified material was used to simulate the protection of paper-based cultural relics, and the synthetic carboxymethyl cellulose fluoride acetate acrylic copolymer lotion was coated on the paper. The research found that the tensile strength of the paper was increased 4.61 times, the water resistance of the paper was also greatly improved, and the reinforcing material had reversibility and certain anti-aging properties [22].

In response to the effect of UV light, graphene has excellent UV protection performance and has been applied in artifact protection in recent years. Graphene is a single-atom layer crystal constructed by hybridizing carbon atoms in  $sp^2$  [23–25]. Because of the transition effect of electrons located in the  $\pi$  state, graphene can absorb UV light in the range of 100–281 nm, exhibit an absorption peak at 250 nm located in the UV light region, and reflect UV light with a wavelength greater than 281 nm [26–28]. However, when graphene oxide is used directly to modify materials because the higher surface energy and van der Waals forces make it less dispersible in the matrix and easy to agglomerate, this greatly reduces the modification effect. Numerous studies have shown that the amino functionalization modification of graphene oxide can improve the dispersity of graphene oxide materials. Meanwhile, more reactive sites are added, which is helpful for strengthening interactions with the polymer matrix. Therefore, it may be able to take advantage of the preventive protection with paper artifacts, thereby weakening the damage of the paper by UV light [29–32].

Based on this, this work utilized aminolated graphene oxide (aGO) as an anti-UV aging agent and carboxymethyl cellulose as a paper reinforcement. The related research of carboxymethylcellulose-amino graphene- composite (CMC-aGO) was expected to provide a theoretical basis for the development of anti-light aging and reinforcement materials for paper relics. The innovations of this work are as follows: (1) Surface modification of CMC with PEI enriches the surface with amino groups and provides an anchoring point for graphene nanosheets; (2) The composite material of graphene and CMC is prepared by simple technology, and the raw material is cheap and easy to obtain, which has practicability and application prospect; (3) The development of reinforcement materials with UV resistance properties enables restorative materials to function as prophylactic protection on the basis of the reinforcement of damaged paper.

## 2. Materials and Methods

### 2.1. Chemicals

CMC, epichlorohydrin, PEI (molecular weight about  $600 \text{ g mol}^{-1}$ ), and KBr were purchased from Shanghai Aladdin Biochemical Technology Co., Ltd. (Shanghai, China). The reagents were all analytical and pure, and the water used for the experiment was deionized water. The simulated pigments (vermilion, malachite, ultramarine, and gamboge), alum gelatin, and rice paper were purchased from Beijing Tianya Pigment Co., Ltd. (Beijing, China).

### 2.2. Preparation of Samples

#### 2.2.1. Synthesis of CMC-aGO

First, 10 mg of GO was added into 140 mL of deionized water, which was pulverized by a homogenizer for 60 min, and ultrasonic dispersion for 30 min to obtain go dispersion with a mass fraction of 6.66%, which was then placed at  $80 \text{ }^{\circ}\text{C}$  for heating. Then, 0.4 g PEI and 0.015 g KOH were added to the above GO dispersion to obtain the GO-PEI mixture by continuous heating and stirring at  $80 \text{ }^{\circ}\text{C}$  for 12 h. Next, 0.1 g CMC was added to the above GO-PEI mixture with stirring for 1 h; then 0.5 g epichlorohydrin was added dropwise to the above reaction system to react at  $80 \text{ }^{\circ}\text{C}$  for 12 h (epichlorohydrin acted as a crosslinking agent [33]). Finally, they were centrifuged, and the obtained solid was washed with ethanol, deionized water repeatedly, and freeze-dried for 48 h. The CMC-GO is directly mixed with CMC and GO, and its proportion is the same as that of CMC-aGO.

#### 2.2.2. Preparation of Simulated Samples

The rice paper was trimmed to the size of 15~240 mm, and the diluted pigments were, respectively, painted evenly on the paper samples, thoroughly shade dried, and protected from light. An amount of 5 mL of the formulated CMC and CMC-aGO dispersions was placed in the spray gun, sprayed evenly on the rice paper with pigments and those without pigments, and placed on the yarn mesh to air dry naturally. These samples were used as simulated samples for the color difference test, tensile strength, and light resistance tests.

### 2.3. Methods of Performance Testing

#### 2.3.1. Instrument Parameter

The molecular structures of CMC, aGO, and CMC-aGO were characterized by Fourier transform infrared spectroscopy. (FTIR, Vertex70, Bruker, Karlsruhe, Germany). Spectral range:  $500\text{--}4000 \text{ cm}^{-1}$ . Scanning electron microscopy (SEM, Hitachi High-tech Co. Ltd., SU-8020, Tokyo, Japan) was used to study the microstructure of the samples. An X-Rite VS450 non-contact spectrophotometer was used to test the color difference of the paper samples.

#### 2.3.2. Dry-Heat Accelerated Aging Experiments

According to GB/T464-2008 (dry heat accelerated aging of paper and cardboard), the paper samples were hung in blueparbho-401, a dry heat aging box, which was set to  $105 \text{ }^{\circ}\text{C}$ , and the aging time was 3 days.

#### 2.3.3. Wet-Heat Accelerated Aging Experiments

According to GB/T22894-2008 (wet heat treatment of accelerated aging of paper and cardboard at  $80 \text{ }^{\circ}\text{C}$  and 65% Relative Humidity), the paper samples were hung up in an HCP wet heat aging box for accelerated aging experiments, which was set at  $80 \text{ }^{\circ}\text{C}$  and 65% relative humidity for 3 days.

#### 2.3.4. UV Aging

The treated samples were placed in a UV aging oven under the following conditions: 40 W power, 313 nm wavelength, and a distance of 50 mm between the surface and the plane of the UV lamp. They were, respectively, irradiated for 3 days, 6 days, and 9 days

and stored in the dark for 24 h for the performance test of paper sample tensile strength testing and color difference.

### 2.3.5. Tensile Strength Testing

Tensile strength testing was used to measure the ability of a paper to resist stretching from external forces. In accordance with GB/T12914-2008 (tensile strength determination of paper and sheets), the measured sheets were cut to size 15 mm × 240 mm. A QT-1136PC universal material testing machine (Xie Qiang Instrument Manufacturing Co. Ltd., Shanghai, China) was used with a tensile rate of 20 mm/min, and the paper was stretched to fracture so that the tensile strength  $S$  (kN/m) was obtained. Tensile strength tests were performed along the transverse and longitudinal sheets, respectively.

### 2.3.6. Color Difference Testing

A CIE  $L \times a \times b$  color coordinate system was used to characterize the color changes before and after paper sample treatment and accelerated aging. The smaller the chromatic difference value ( $\Delta E$ ) of the paper represents, the smaller the color change before and after sample reinforcement and accelerated aging. The CIE  $L \times a \times b$  color system chromatic difference value is calculated as follows:

$$\Delta E = [(\Delta L)^2 + (\Delta a)^2 + (\Delta b)^2]^{1/2}$$

Among them,  $\Delta L$  represents the difference in light acuity,  $\Delta a$  represents the red green deviation, and  $\Delta b$  represents the yellow blue deviation [34].

## 3. Results

### 3.1. Characterization of CMC-aGO

The present work was intended to proceed through the synthesis of CMC-aGO (Figure 1). On the one hand, carboxymethyl cellulose cross-links with the inner fiber of the paper, which in turn achieves the effect of fill reinforcement. On the other hand, the polyethyleneimine (PEI)-modified graphene oxide surface contains a high density of amino groups, which easily form bonds with the cellulose surface carboxymethyl, such that GO nanosheets adhere to the cellulose surface; the introduction of graphene can achieve the effect of protecting against UV light.

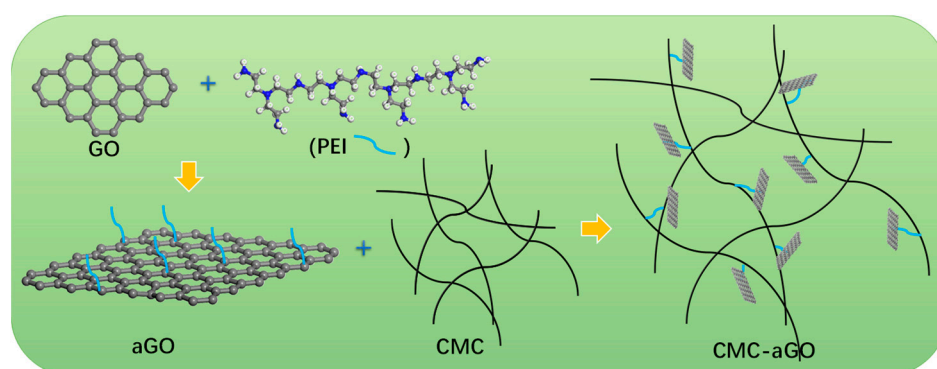


**Figure 1.** Schematic of the synthetic procedure for CMC-aGO.

The microtopography of CMC-aGO was observed by SEM. As shown in Figure 2a, CMC-aGO consisted of a large number of nanofibers with diameters of ~10 nm. The nanofibers were randomly arranged and overlapped to form a coherent three-dimensional porous network structure. The GO layers are closely bonded to a large number of BC nanofibers without agglomeration (as shown in the color block diagrams of Figure 2a). In terms of macroscopic morphology, CMC-aGO was uniformly dispersed after 12 h rest.

However, the CMC-GO, which directly mixes GO and CMC, was obviously separated (Figure 2b).

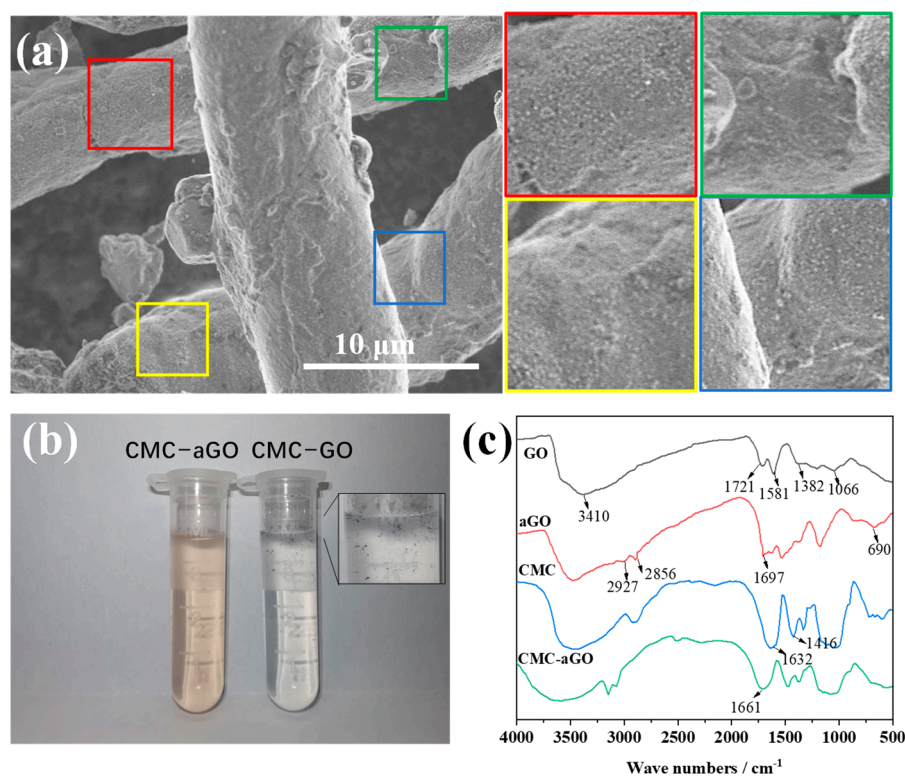


**Figure 2.** (a) SEM of CMC-aGO (Colored blocks on the right are local magnifications); (b) Photo of CMC-aGO and CMC-GO; (c) FT-IR of GO, aGO, CMC, and CMC-aGO.

Then, in order to further verify the interaction between graphene, PEI, and cellulose, a series of materials were tested by FT-IR. Figure 2c shows the FT-IR diagrams of GO, aGO, CMC, and CMC-aGO. The absorption peaks of GO at 1066, 1381, 1581, and 1721 cm<sup>-1</sup> were, respectively, generated by C=O, C-OH, C=C, and C-O-C vibration. The wider absorption peak at 3410 cm<sup>-1</sup> is the expansion vibration of -OH. The absorption peaks of PEI-modified GO at 2856 and 2927 cm<sup>-1</sup> were caused by the C-H tensile vibration of aliphatic and aromatic groups, and the characteristic peaks at 1697 and 669 cm<sup>-1</sup> were caused by N-H bending and swinging, respectively. This was caused by the amidation reaction between amino groups in PEI and carboxyl groups on the GO surface, which indicates that PEI was modified on the GO surface. The peaks of CMC at 1632 cm<sup>-1</sup> and 1416 cm<sup>-1</sup> are asymmetric and symmetric expansion vibration absorption peaks of -COOH, respectively. The FT-IR spectra of CMC-aGO show that the N-H characteristic peak disappeared and the characteristic peak of -COOH decreased. The absorption peak at 1661 cm<sup>-1</sup> may be due to the amidation of -CONH- between -NH<sub>2</sub> in PEI and -COOH in CMC or GO, which indicates that GO and PEI successfully grafted onto the CMC surface [35,36].

The micromorphology of the paper cultural relics is shown in Figure 3a, the paper fibers are intertwined, and there are a large number of voids among the fibers. Excellent reinforcing materials can penetrate into the voids between the fibers and cross-link with the internal fibers of the paper to achieve the effect of filling and reinforcing. There were obvious deterioration signs, such as the breakage and fracture of the paper fiber before reinforcement, and a large number of voids exist among the fibers (Figure 3a, red dotted circle marker in Figure 3a). After CMC-aGO reinforcement, the CMC fibers formed cross-linking structures between the paper fibers, which reduced the porosity of the paper samples and reinforced the fragile paper (Figure 3b). SEM showed that the size of paper

fibers did not change significantly before and after CMC repair, and the surface of the repaired sample was smooth.

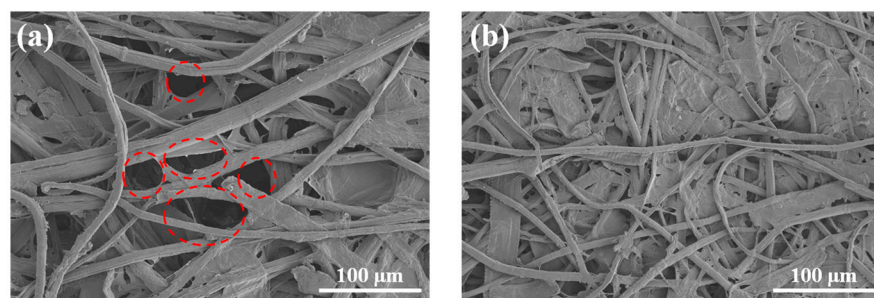


**Figure 3.** SEM of (a) Paper fibers; (b) Paper fiber reinforcement by CMC-aGO. (red circles represent interfibrillar voids).

### 3.2. Performance Characterization of CMC-aGO

The color change is an important indicator to evaluate the suitability of reinforcement materials for paper reinforcement. The color difference measurements of the paper and pigments before and after reinforcement were tested. As shown in Figure 4a, the color difference of the paper changed after being treated with CMC and CMC-aGO. After CMC and CMC-aGO treatment, the paper color difference values were 1.3 and 1.5, respectively, and the color difference standard ( $\Delta E = 3$ ) was less than three, which belonged to the range of color difference tolerance. It shows that CMC had no significant effect on the original appearance of the paper. Then, the color difference effects of the four pigments under the reinforcement of CMC and CMC-aGO were tested. As shown in Figure 4b, the influence of CMC and CMC-aGO on the color difference of vermilion, malachite, ultramarine, and gamboge pigments were studied. After the minor addition of graphene was added, the  $\Delta E$  of vermilion and malachite samples treated by CMC-aGO were 2.3 and 2.2, respectively, which is slightly higher than that of the samples treated by CMC. However, an  $\Delta E$  less than three belonged to the range of color difference tolerance. The color difference between CMC-aGO on ultramarine and gamboge was less than that of CMC, and the effect of pure color was obvious. The results showed that the addition of a small amount of graphene did not cause any change in the color difference between the paper and pigment.

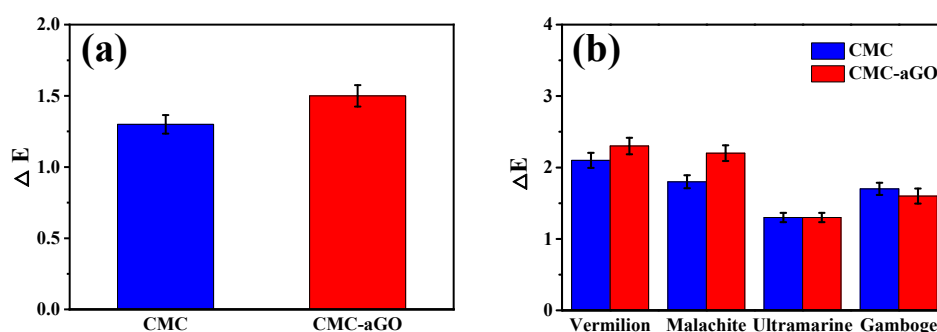


**Figure 4.** The color difference of (a) The paper and (b) Pigments before and after reinforcement.

The tensile strength of paper is one of the important indexes to evaluate the physical performance of the paper. CMC and CMC-aGO were used to reinforce the rice paper, while the alum gelatin was used as a control. The tensile strength test results of the paper after reinforcement are shown in Figure 5; the tensile strength of the paper after reinforcement with alum gelatin, CMC and CMC-aGO was significantly larger compared to that of the untreated rice paper. Among them, CMC-aGO showed the most excellent performance with a tensile strength of 2.2 kN/m and 2.9 kN/m in the cross and machine direction, which

were significantly better than alum gelatin (1.4 kN/m, 2.3 kN/m) and CMC (1.7 kN/m, 2.6 kN/m).

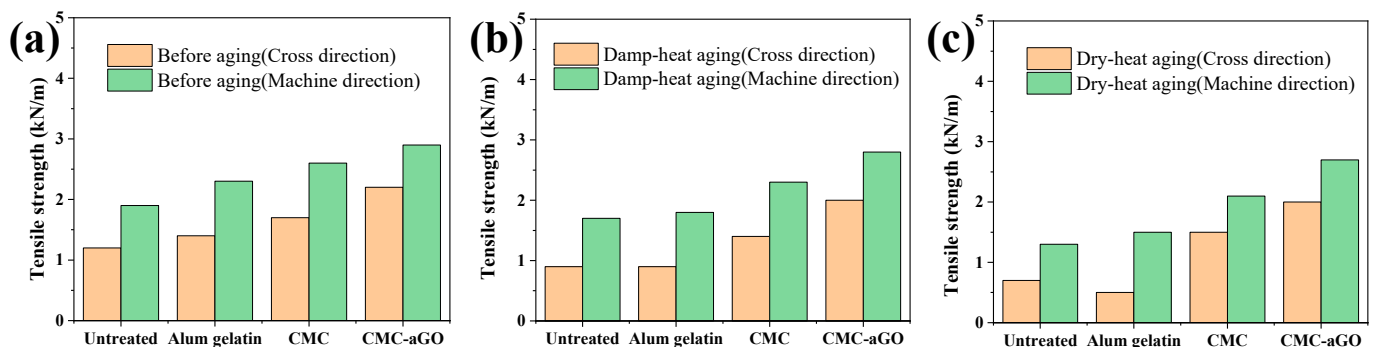


**Figure 5.** Tensile Strength of paper (a) Before aging, (b) After damp-heat aging, and (c) Dry-heat aging.

Then, dry heat aging and wet heat aging treatments were performed on the paper treated with different reinforcement agents. The results showed that, compared with the blank samples, CMC-aGO-treated samples were least affected by dry-heat aging and wet-heat aging, and the samples treated with alum had the greatest influence. After dry heat aging, the cross-direction strength and machine direction of CMC-aGO treated samples decreased by 9% and 6.9%, respectively, and after wet-heat aging, the cross and machine direction strength decreased by 9% and 3.4%, respectively. While significantly better than CMC, this may have been due to the interactions between the aGO and CMC with the paper fiber, the oxygen-containing groups, and hydrogen bonds in the CMC aGO interacting with the paper cellulose, thus enabling the formation of the stable fibrous network on the surface of the paper, and achieving the filling reinforcement at the damaged paper fiber pores and fracture sites, increasing the strength and toughness of the fibers, and reinforcement of the paper.

The reinforcement mechanism was analyzed. The paper fiber strength and the binding strength between the fibers are the main factors that affect the paper's mechanical strength. Fiber length and fiber interlacing factors also contribute to the paper's mechanical strength. These factors affect the strength performance index of the paper in a complex way, such as the tensile strength, the number of folds, and tear strength. Usually, the binding strength between cellulose is the most dominant influencing factor. After CMC treatment, the inter-fiber bonding strength is strengthened.

Some pigments are prone to photo-oxidation reaction under UV light, which excites the double bond of part of the excited state to react with the oxygen in the air, leading to a change in pigment color, a faded appearance, and a discoloration phenomenon. To explore the UV light-resistant properties of reinforcement materials, a series of tests were carried out. It is known from Figure 6a that the pigment color difference value  $\Delta E$  of each group remained largely unchanged after 90 days of UV aging for CMC-aGO treated samples compared to CMC-treated samples during the UV aging test. Among them, CMC-aGO showed the best color fixation effect on vermilion and gamboge. The CMC-treated samples showed more variable color difference values starting from 30 days, all of which exceeded the values of  $\Delta E = 3$ , especially for the vermilion pigment. This phenomenon might be attributed to the lack of UV resistance properties in CMC materials, and the vermilion was prone to crystal phase transition to beta-mercury sulfide ( $\beta$ -HgS) under UV light conditions. Ultraviolet light has higher energy than is required for crystal phase transformation, which can make the cinnabar crystal phase change rapidly and color become darker. Graphene in CMC-aGO absorbs some ultraviolet rays, effectively delaying the damage caused by ultraviolet rays.

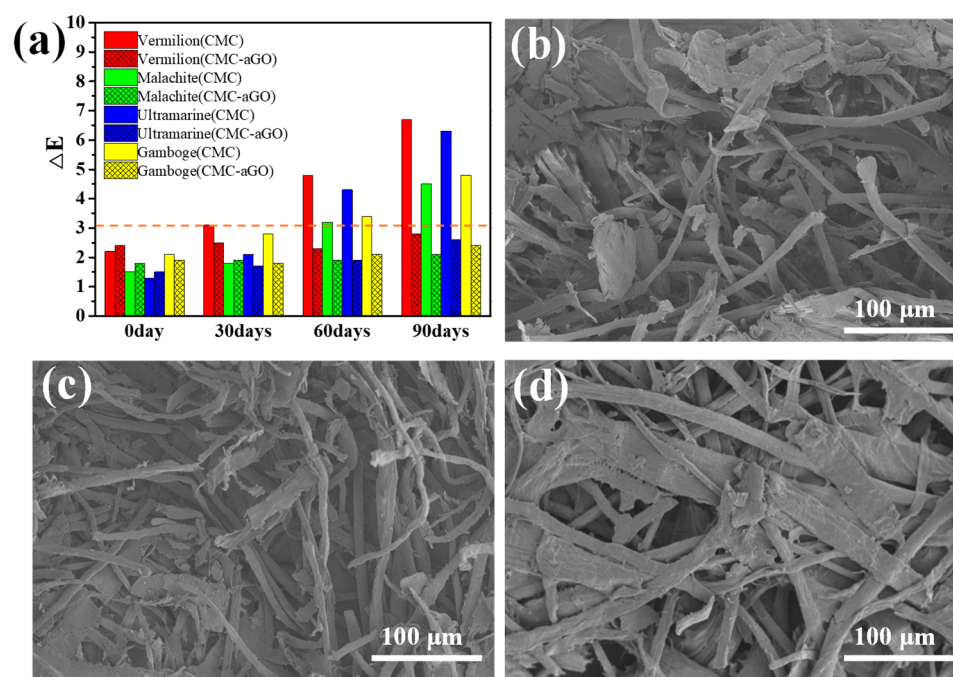


**Figure 6.** (a) Color difference of four pigments treated with CMC and CMC-aGO after UV aging. SEM of (b) The blank group, (c) CMC, and (d) CMC-aGO-treated paper after UV aging.

The microstructure test results show that (Figure 6b–d) some fiber structure breakage occurred after aging, among which, the damaged fibers of the blank group (Figure 6b) and CMC (Figure 6c) were more serious after aging. While the CMC-aGO-treated samples largely kept their fibrous structures intact after UV aging, only a few fiber fracture phenomena appeared. This phenomenon further confirmed the anti-UV effect of GO in CMC-aGO.

#### 4. Conclusions

In summary, CMC with aminolated graphene oxide composites was successfully synthesized by a simple synthetic method, which was applied with paper reinforcement and protection against UV light. The results show that the PEI-modified aGO surface contains high-density amino groups, which are easy to bond with carboxymethyl groups on the surface of cellulose. Graphene nano-sheets adhere to the surface of cellulose and effectively improve the dispersion of graphene in the water. CMC in the composite materials crosslinks with the fibers inside the paper to achieve filling and reinforcement effects, and GO in the composite materials has an anti-ultraviolet effect. By testing the color difference in paper reinforcement and pigments, it is shown that the appearance of paper cultural relics was not affected by the small amount of graphene added. The reinforcement and ultraviolet resistance of CMC-aGO were verified by tensile tests and simulated aging tests. The development of CMC-aGO has great application potential in the protection of cultural heritage and is of great significance to the development of paper conservation materials.

**Author Contributions:** Conceptualization, P.T.; Methodology, M.S.; Investigation, J.H.; Writing—original draft, P.F. All authors have read and agreed to the published version of the manuscript.

**Funding:** This research received no external funding.

**Institutional Review Board Statement:** Not applicable.

**Informed Consent Statement:** Not applicable.

**Data Availability Statement:** Not applicable.

**Conflicts of Interest:** The authors declare no conflict of interest.

## References

1. He, B.; Lin, Q.X.; Chang, M.M.; Liu, C.F.; Fan, H.M.; Ren, J.L. A new and highly efficient conservation treatment for deacidification and strengthening of aging paper by in-situ quaternization. *Carbohydr. Polym.* **2019**, *209*, 250–257. [[CrossRef](#)] [[PubMed](#)]
2. Zervos, S.; Alexopoulou, I. Paper conservation methods: A literature review. *Cellulose* **2015**, *22*, 2859–2897. [[CrossRef](#)]
3. Barnat-Hunek, D.; Grzegorzczak-Franczak, M.; Klimek, B.; Pavlikova, M.; Pavlik, Z. Properties of multi-layer renders with fly ash and boiler slag admixtures for salt-laden masonry. *Constr. Build. Mater.* **2021**, *278*, 122366. [[CrossRef](#)]
4. Noake, E.; Lau, D.; Nel, P. Identification of cellulose nitrate based adhesive repairs in archaeological pottery of the university of melbourne's middle eastern archaeological pottery collection using portable ftir-atr spectroscopy and pca. *Herit. Sci.* **2017**, *5*, 3. [[CrossRef](#)]
5. Akyuz, T.; Akyuz, S.; Balci, K.; Gulec, A. Investigations of historical textiles from the imperial pavilion (hunkar kasri) of the new mosque eminonu-istanbul (turkey) by multiple analytical techniques. *J. Cult. Herit.* **2017**, *25*, 180–184. [[CrossRef](#)]
6. Bertolini, L.; Carsana, M.; Redaelli, E. Conservation of historical reinforced concrete structures damaged by carbonation induced corrosion by means of electrochemical realkalisation. *J. Cult. Herit.* **2008**, *9*, 376–385. [[CrossRef](#)]
7. Gorassini, A.; Adami, G.; Calvini, P.; Giacomello, A. Atr-ftir characterization of old pressure sensitive adhesive tapes in historic papers. *J. Cult. Herit.* **2016**, *21*, 775–785. [[CrossRef](#)]
8. Havlinova, B.; Katuscak, S.; Petrovicova, M.; Makova, A.; Brezova, V. A study of mechanical properties of papers exposed to various methods of accelerated ageing. Part I: The effect of heat and humidity on original wood-pulp papers. *J. Cult. Herit.* **2009**, *10*, 222–231. [[CrossRef](#)]
9. Yang, Z.H.; Zhang, J.J.; Qi, Y.P.; Shen, Y.F.; Li, H. Application of hydrophobically modified hydroxyethyl cellulose-methyl methacrylate copolymer emulsion in paper protection. *Nord. Pulp. Pap. Res. J.* **2022**, *37*, 282–289. [[CrossRef](#)]
10. Wu, X.; Mou, H.Y.; Fan, H.M.; Yin, J.Y.; Liu, Y.B.; Liu, J.A. Improving the flexibility and durability of aged paper with bacterial cellulose. *Mater. Today Commun.* **2022**, *32*, 103827. [[CrossRef](#)]
11. Shehata, M.; Navarra, M.; Klement, T.; Lachemi, M.; Schell, H. Use of wet cellulose to cure shotcrete repairs on bridge soffits. Part 1: Field trial and observations. *Can. J. Civ. Eng.* **2006**, *33*, 807–814. [[CrossRef](#)]
12. Luo, Y.B. Durability of chinese repair bamboo papers under artificial aging conditions. *Stud. Conserv.* **2019**, *64*, 448–455. [[CrossRef](#)]
13. Henniges, U.; Angelova, L.; Schwoll, S.; Smith, H.; Bruckle, I. Microfibrillated cellulose films for mending translucent paper: An assessment of film preparation and treatment application options. *J. Inst. Conserv.* **2022**, *45*, 36–51. [[CrossRef](#)]
14. Fu, L.N.; Zhang, J.; Yang, G. Present status and applications of bacterial cellulose-based materials for skin tissue repair. *Carbohydr. Polym.* **2013**, *92*, 1432–1442. [[CrossRef](#)]
15. Egertsdotter, E.M.U.; Aidun, C.K. Renewable materials for tissue repair/biocompatibility of cellulose nanocrystals. In Proceedings of the 5th IASTED International Conference on Biomedical Engineering, Innsbruck, Austria, 14–16 February 2007.
16. Dadabayev, R.; Malka, D. A visible light rgb wavelength demultiplexer based on polycarbonate multicore polymer optical fiber. *Opt. Laser Technol.* **2019**, *116*, 239–245. [[CrossRef](#)]
17. Gelkop, B.; Aichnboim, L.; Malka, D. Rgb wavelength multiplexer based on polycarbonate multicore polymer optical fiber. *Opt. Fiber Technol.* **2021**, *61*, 102441. [[CrossRef](#)]
18. Borges, I.D.; Casimiro, M.H.; Macedo, M.F.; Sequeira, S.O. Adhesives used in paper conservation: Chemical stability and fungal bioreceptivity. *J. Cult. Herit.* **2018**, *34*, 53–60. [[CrossRef](#)]
19. Rahman, M.S.; Hasan, M.S.; Nitai, A.S.; Nam, S.; Karmakar, A.K.; Ahsan, M.S.; Shiddiky, M.J.; Ahmed, M.B.J.P. Recent developments of carboxymethyl cellulose. *Polymers* **2021**, *13*, 1345. [[CrossRef](#)]
20. Sanchez, E.; Sanz, V.; Bou, E.; Monfort, E. Carboxymethylcellulose used in ceramic glazes part iii: Influence of cmc characteristics on glaze slip and consolidated glaze layer properties. *Cfi-Ceram. Forum Int.* **1999**, *76*, 24–27.
21. Petrea, P.; Ciolacu, F.; Ciovica, S. The evaluation of some consolidation agents applied in the conservation of graphical documents. *Eur. J. Sci. Theol.* **2010**, *6*, 67–75.
22. Chen, Q.; Wen, W.-Y.; Qiu, F.-X.; Xu, J.-C.; Yu, H.-Q.; Chen, M.-L.; Yang, D.-Y. Preparation and application of modified carboxymethyl cellulose si/polyacrylate protective coating material for paper relics. *J. Chem. Pap.* **2016**, *70*, 946–959. [[CrossRef](#)]
23. Farivar, F.; Yap, P.L.; Tung, T.T.; Losic, D. Highly water dispersible functionalized graphene by thermal thiolene click chemistry. *Materials* **2021**, *14*, 2830. [[CrossRef](#)] [[PubMed](#)]
24. Costa, M.C.F.; Marangoni, V.S.; Ng, P.R.; Nguyen, H.T.L.; Carvalho, A.; Neto, A.H.C. Accelerated synthesis of graphene oxide from graphene. *Nanomaterials* **2021**, *11*, 551. [[CrossRef](#)] [[PubMed](#)]
25. Binder, J.; Rogoza, J.; Tkachenko, L.; Pasternak, I.; Sitek, J.; Strupinski, W.; Zdrojek, M.; Baranowski, J.M.; Stepniewski, R.; Wismolek, A. Suspended graphene on germanium: Selective local etching via laser-induced photocorrosion of germanium. *2D Mater.* **2021**, *8*, 035043. [[CrossRef](#)]
26. Rochford, C.; Kumar, N.; Liu, J.W.; Zhao, H.; Wu, J. All-optical technique to correlate defect structure and carrier transport in transferred graphene films. *ACS Appl. Mater. Inter.* **2013**, *5*, 7176–7180. [[CrossRef](#)]
27. Duong, D.L.; Han, G.H.; Lee, S.M.; Gunes, F.; Kim, E.S.; Kim, S.T.; Kim, H.; Ta, Q.H.; So, K.P.; Yoon, S.J.; et al. Probing graphene grain boundaries with optical microscopy. *Nature* **2012**, *490*, 235–239. [[CrossRef](#)]
28. Chen, Z.Y.; Zhang, Y.H.; Zhang, H.R.; Sui, Y.P.; Zhang, Y.Q.; Yu, G.H.; Jin, Z.; Liu, X.Y. Probing graphene grain boundaries and enhancing the electrical properties of graphene films by pt modification. *Mater. Lett.* **2014**, *131*, 53–56. [[CrossRef](#)]

29. Saladino, M.L.; Markowska, M.; Carmone, C.; Cancemi, P.; Alduina, R.; Presentato, A.; Scaffaro, R.; Bialy, D.; Hasiak, M.; Hreniak, D.; et al. Graphene oxide carboxymethylcellulose nanocomposite for dressing materials. *Materials* **2020**, *13*, 1980. [[CrossRef](#)]
30. Ponnuchamy, V.; Esakkimuthu, E.S. Density functional theory study of lignin, carboxymethylcellulose and unsustainable binders with graphene for electrodes in lithium-ion batteries. *Appl. Surf. Sci.* **2022**, *573*, 151461. [[CrossRef](#)]
31. Karimzadeh, Z.; Javanbakht, S.; Namazi, H. Carboxymethylcellulose/mof-5/graphene oxide bio-nanocomposite as antibacterial drug nanocarrier agent. *Bioimpacts* **2019**, *9*, 5–13. [[CrossRef](#)]
32. Araque, E.; Villalonga, R.; Gamella, M.; Martinez-Ruiz, P.; Sanchez, A.; Garcia-Baonza, V.; Pingarron, J.M. Water-soluble reduced graphene oxide-carboxymethylcellulose hybrid nanomaterial for electrochemical biosensor design. *ChemPlusChem* **2014**, *79*, 1334–1341. [[CrossRef](#)]
33. Guan, H.; Li, J.; Zhang, B.; Yu, X. Synthesis, properties, and humidity resistance enhancement of biodegradable cellulose-containing superabsorbent polymer. *J. Polym.* **2017**, *2017*, 3134681. [[CrossRef](#)]
34. Bourguignon, E.; Tomasin, P.; Detalle, V.; Vallet, J.-M.; Labouré, M.; Olteanu, I.; Favaro, M.; Chiurato, M.A.; Bernardi, A.; Becherini, F. Calcium alkoxides as alternative consolidants for wall paintings: Evaluation of their performance in laboratory and on site, on model and original samples, in comparison to conventional products. *J. Cult. Herit.* **2018**, *29*, 54–66. [[CrossRef](#)]
35. Yang, G.; Cao, J.; Li, L.; Rana, R.K.; Zhu, J.-J. Carboxymethyl chitosan-functionalized graphene for label-free electrochemical cytosensing. *Carbon* **2013**, *51*, 124–133. [[CrossRef](#)]
36. Singh, A.; Yadagiri, G.; Negi, M.; Kushwaha, A.K.; Singh, O.P.; Sundar, S.; Mudavath, S.L.J.I.J.o.B.M. Carboxymethyl chitosan modified lipid nanoformulations as a highly efficacious and biocompatible oral anti-leishmanial drug carrier system. *Int. J. Biol. Macromol.* **2022**, *204*, 373–385. [[CrossRef](#)]

**Disclaimer/Publisher’s Note:** The statements, opinions and data contained in all publications are solely those of the individual author(s) and contributor(s) and not of MDPI and/or the editor(s). MDPI and/or the editor(s) disclaim responsibility for any injury to people or property resulting from any ideas, methods, instructions or products referred to in the content.